CRYSTALLINE MICROSTRUCTURE ROLE IN THE HIGH FIELD Q-SLOPE*

A. Romanenko†, CLASSE, Ithaca, NY, USA

Abstract

Samples, which were cut out from high field Q-slope limited small and large grain BCP- and EP-treated niobium cavities, were analyzed using EBSD, FIB/TEM, and EELS. Dislocation density maps were obtained from raw EBSD data based on the procedure outlined in [1, 2]. Subsequent vacuum annealing of samples at 100-120°C resulted in an observable change in the geometrically necessary dislocation density in large grain BCP and small grain EP samples. TEM images of the samples prepared by FIB did not reveal any observable differences in the oxide/metal interface structure. In addition, no suboxide clusters, cracks or other interface irregularities were observed in both baked and unbaked samples. EELS analysis of the elemental composition revealed about 5 nanometers of oxide followed by a sharp decrease of the oxygen signal with no extended layer of significant oxygen content. MCR analysis of EELS data showed that the best fit is provided by three components: niobium pentoxide, interfacial layer of an intermediate Nb oxidation state and bulk niobium. Mild baking followed by the air exposure for a few weeks did not result in any changes in the Nb and O signals as deduced from EELS data. A new possible explanation for the HFQS based on dislocations as premature flux entry sites is suggested. Mild baking effect is proposed to be due to dislocation density reduction enabled by vacancy-assisted dislocation climb.

INTRODUCTION

The origin of the high field Q-slope (HFQS) in SRF niobium cavities remains to be unclear, although many models were proposed over the last few years. One of the major obstacles for understanding the effect is a lack of detailed physical knowledge about niobium surface structure. The key hint to understanding the HFQS is the mild baking effect. Mild baking is a UHV annealing of a cavity at 100-120°C for 1-2 days depending on the grain size. Applying mild baking to HFQS-limited cavities eliminates the HFQS in electropolished and large grain BCP cavities, and might in some cases improve the performance of small grain BCP cavities. A physical mechanism, which underlies changes in niobium properties due to baking, is unknown.

Up to now, the focus of surface studies was mostly on interstitial impurities (oxygen, hydrogen, nitrogen etc.) and on the oxide structure. It was motivated by the calculated oxygen diffusion length in niobium (a few tens of nanometers for two days baking period), which roughly agrees with the thickness of a baking-modified layer, and by the strong effect interstitial oxygen has on superconducting properties of niobium. In this contribution we report results for crystalline lattice microstructure in the context of the HFQS, which was not previously studied.

Samples used throughout this project were dissected from hot and cold areas identified with thermometry in the HFQS-limited cavities. For clarity, areas, which exhibited stronger (weaker) HFQS and consequently stronger (weaker) RF dissipation, will be called hot (cold) spots. Details on cavity tests, thermometry, and cavity dissection are reported elsewhere [3, 4]. In this particular contribution we analyze samples from small grain (about 1 mm) BCP and EP cavities and large grain (tens of centimeters) BCP cavity.

In the first part of this study we investigated a surface dislocation structure of niobium cavity samples before and after mild baking utilizing EBSD mapping.

In the second part of the investigations we analyzed niobium surface structure within the penetration depth using FIB-prepared samples from hot and cold spots. TEM/STEM was used for atomic scale imaging, and electron energy loss spectroscopy (EELS) provided a nanometer scale elemental analysis.

EBSD RESULTS

Cornell Center for Materials Research Leica 440 SEM equipped with the HKL Nordlys detector for EBSD measurements was used for data acquisition. HKL software was used for data processing and local misorientation calculations. The information depth for EBSD is about 50-100 nm for niobium, which is comparable to both coherence length $\xi \approx 40\ nm$ and London penetration depth $\lambda \approx 40\ nm$. Hence, the information obtained directly characterizes the near-surface region, which is relevant for the RF performance.

In the first part of this study, crystalline orientation maps with a 1-2 μm step size were obtained for hot and cold spots. After the crystalline orientation maps were obtained, *local misorientation* maps were calculated from them. A local misorientation (LM) at a pixel is defined as an average misorientation (in degrees throughout this contribution) between the pixel and its neighbors. Thus, LM is a measure of a local crystalline lattice distortion, which should be intimately related to dislocations since dislocations accommodate plastic deformations. In Fig. 1 LM distributions for small grain BCP, large grain BCP, and small grain EP cases are shown. From the plots the LM is on average shifted toward higher angles in hot spots as compared to cold spots. Magnitude of the shift is strongest in large grain BCP sam-

* Work supported by NSF
† aroman@fnal.gov

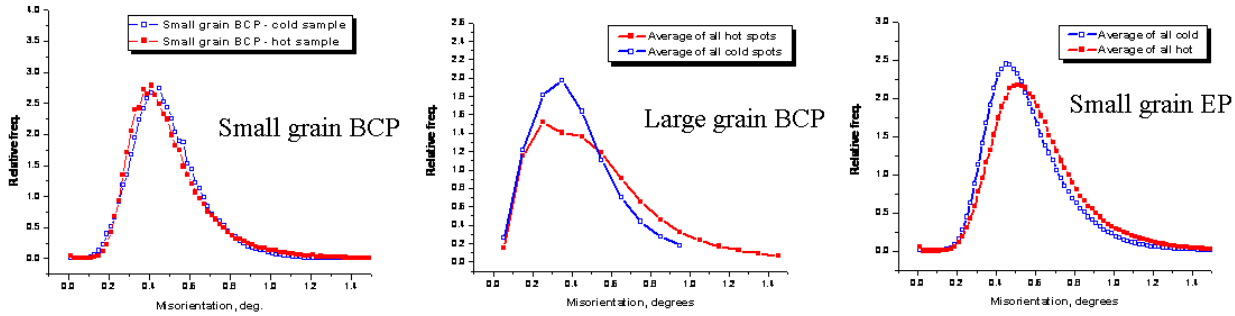

Figure 1: Local misorientation distributions for hot and cold spots in small grain BCP (left), large grain BCP (center), and small grain EP (right) cavities.

ples, whereas small grain EP and BCP samples exhibit a weak shift.

In the second part of the study, a few samples from each type were baked at 120°C (mild baking) for about 2 days and reanalyzed with EBSD in order to look for any changes. Comparisons of LM distributions before and after mild baking are shown in Fig. 3–4. In the small grain BCP case there is almost no change observed. Mild baking of the large grain BCP sample shifted LM distribution to lower angles. Finally, in the case of the small grain EP both hot and cold samples exhibited a significant shift toward lower LM angles.

Having obtained crystalline orientation maps of the sample surface, it is possible to extract dislocation density distributions from them following the procedure outlined in [1, 2]. As a result, a lower bound estimate on the dislocation densities of pure screw and edge types can be extracted. For two hot and cold spots from the small grain EP cavity, a dislocation density tensor components were calculated. In Fig. 5 an average of 4 pure screw dislocation types is shown for hot and cold samples before and after mild baking. In Fig. 6 a distribution of 12 pure edge dislocation density is presented. An average dislocation density is defined as

$$\rho_{avg} = \sqrt{\sum_i \rho_i^2}$$

where sum is taken over i types of dislocations (4 for screw and 12 for edge). An absolute value of average dislocation density for not baked samples was of order $10^{10}\ m^{-2}$, which would be helpful for later discussion.

Both local misorientation distributions and calculated dislocation density maps show mild difference between hot and cold spots before baking, with the strongest difference observed in the large grain BCP case followed by milder difference in small grain BCP and EP cases. A relative magnitude of the difference is consistent with thermometry data (for details see [4]), which shows that large grain BCP cavities have the strongest temperature difference between hot and cold spots at highest achievable fields. Small grain BCP and EP cavities, on the other hand, exhibit a relatively mild difference between hot and cold spots, which is the case for dislocation densities as well.

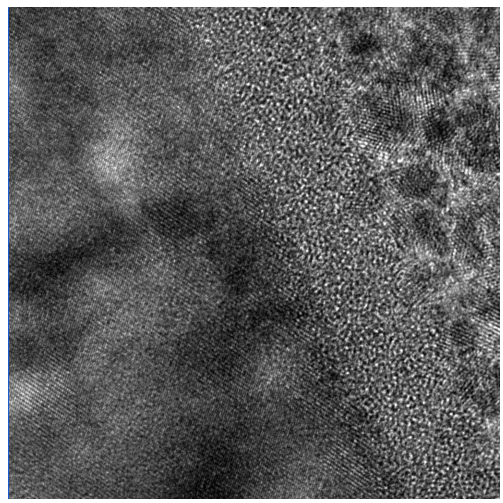

Figure 2: Typical TEM bright field micrograph of the hot spot sample (image obtained by P. Ercius). From left to right on the micrograph: crystalline bulk Nb, amorphous Nb oxide, polycrystalline Pt protective layer.

Another apparent conclusion, which is not obvious from local misorientation distributions, is the cell-like distribution of dislocations visible in both screw and edge dislocation density maps. The typical size of each cell from Fig. 5- 6 is about a few tens of micrometers.

After mild baking of small grain EP samples, a significant decrease in both screw and edge dislocation densities is observed. In the large grain BCP case the change due to baking is strong as well. This correlates well with the experimental fact that all EP and large grain BCP cavities are free of the HFQS after mild baking is applied. Small grain BCP cavities, on the other hand, do not respond consistently to mild baking. In some cases an improvement in the HFQS onset field or the HFQS severity is observed, while in other cases no benefit is attained. And, again, in good correlation with cavity experiments, local misorientations and dislocation densities almost do not change for small grain BCP samples.

FIB/TEM AND EELS RESULTS

In order to prepare samples for TEM/STEM and EELS investigations FEI Strata 400 STEM/FIB system was used.

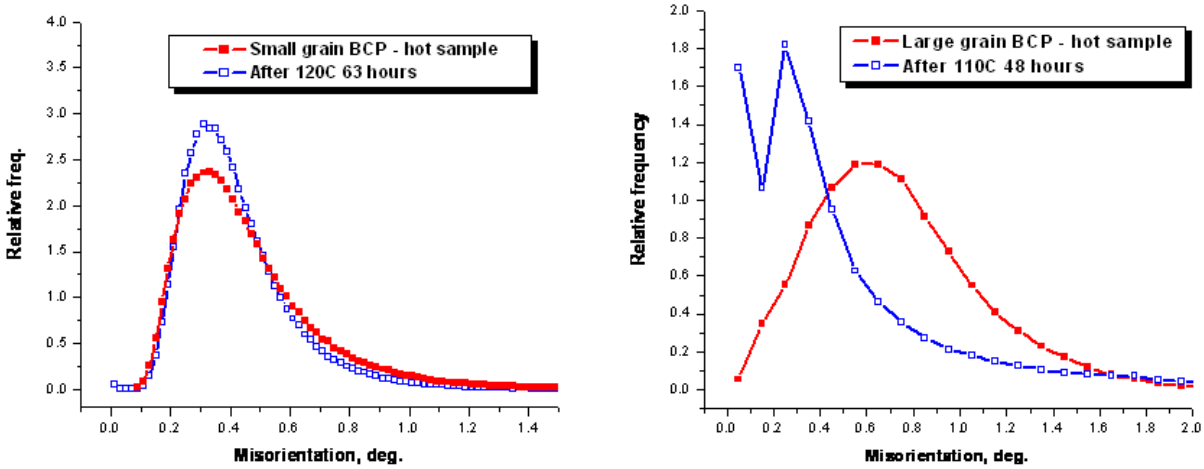

Figure 3: Local misorientation distributions for small and large grain BCP samples before and after mild baking.

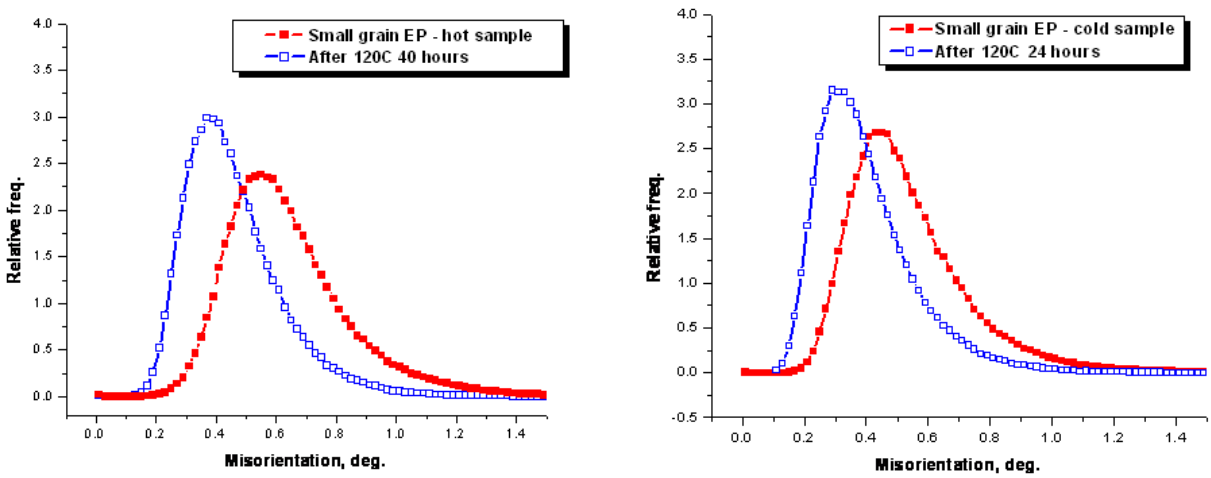

Figure 4: Local misorientation distributions for small grain EP samples before and after mild baking.

Before any ion milling was applied, a protective layer of platinum (Pt) was deposited by an e-beam, followed by the ion beam deposition of an additional platinum layer. Thickness of the e-beam deposited platinum was about 100 nm, and the ion-beam deposited layer was about 1 μm thick. Two samples from the small grain EP cavity were prepared by FIB: one from the hot spot as is, and one from another hot spot after mild baking.

FEI Tecnai G2 F20 TEM/STEM system equipped with EELS capable of atomic scale imaging and chemical analysis was used for sample studies. Typical TEM micrographs obtained on both samples are shown in Fig. 2. Images do not reveal any visual difference in the oxide, interface or bulk structure between the samples. Polycrystalline platinum layer is followed by the amorphous homogeneous niobium oxide layer about 5 nm thick. At and nearby interface no layers of different nature are observed, such as suboxide layers or clusters. Underneath an amorphous niobium oxide a crystalline structure of bulk niobium is clearly visible.

EELS data was obtained by getting line profiles across the Pt/oxide/bulk structure with steps below 1 nm around Nb-$M_{2,3}$ and O-K edges. Data analysis was performed using the Multivariate Curve resolution (MCR) method in order to get a number of components in the oxide needed to fit the spectra.

Depth profiles of Nb and O EELS signals for baked and unbaked samples are shown in Fig. 7. Niobium and oxygen concentrations shown in these graphs are in arbitrary units. Distributions of both Nb and O signals with depth look the same for both baked and unbaked samples that means that the oxide structure does not change with baking and distribution of interstitial oxygen (on the level of EELS resolution) does not change as well.

Results of the MCR decomposition for the unbaked hot spot sample of Nb-$M_{2,3}$ spectral line show that the best fit to the signal is provided by three components, and by two components in O-K signal as shown in Fig. 8. Comparing the MCR components to reference spectra from [5] the components correspond to niobium in Nb_2O_5, niobium in intermediate oxidation state $NbO_x, 1 < x < 2$, and bulk niobium.

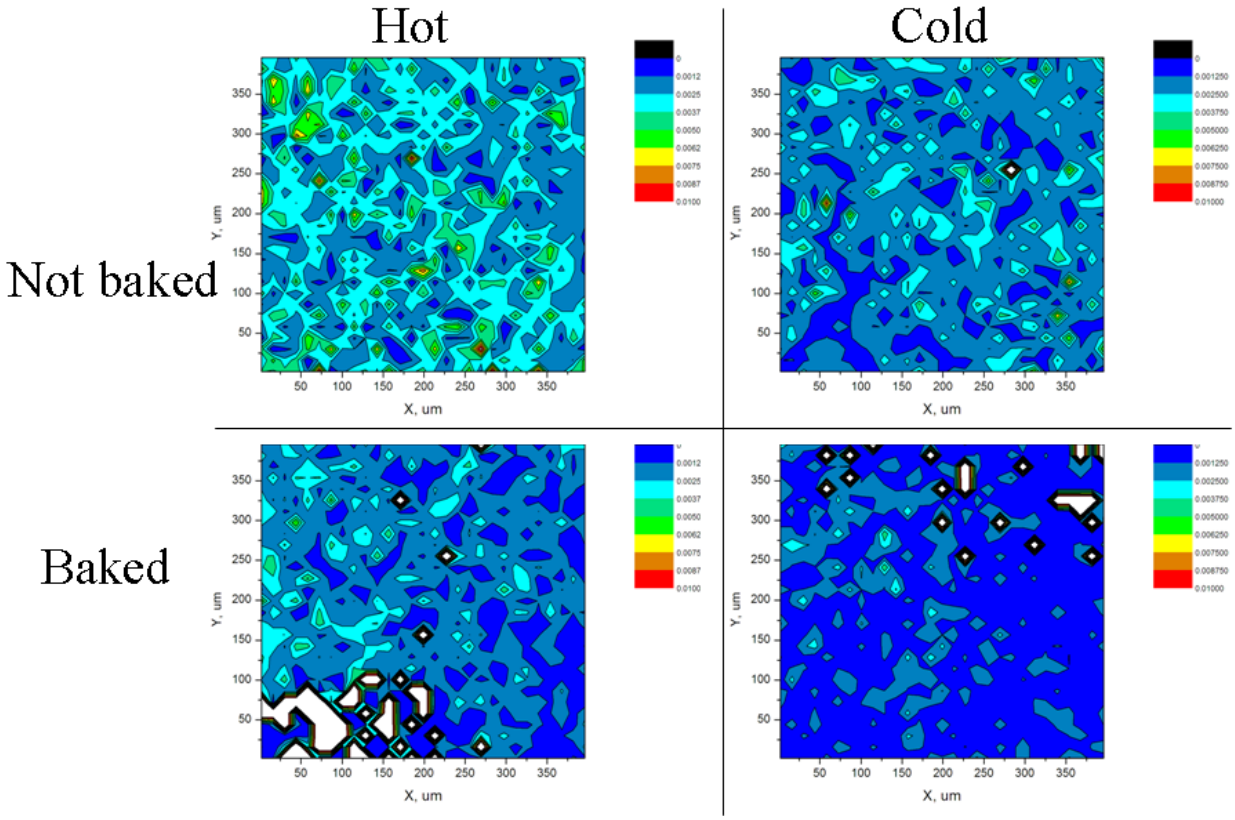

Figure 5: Average screw dislocation density (in arbitrary units) for hot (left column) and cold (right column) spots before (top row) and after (bottom row) mild baking.

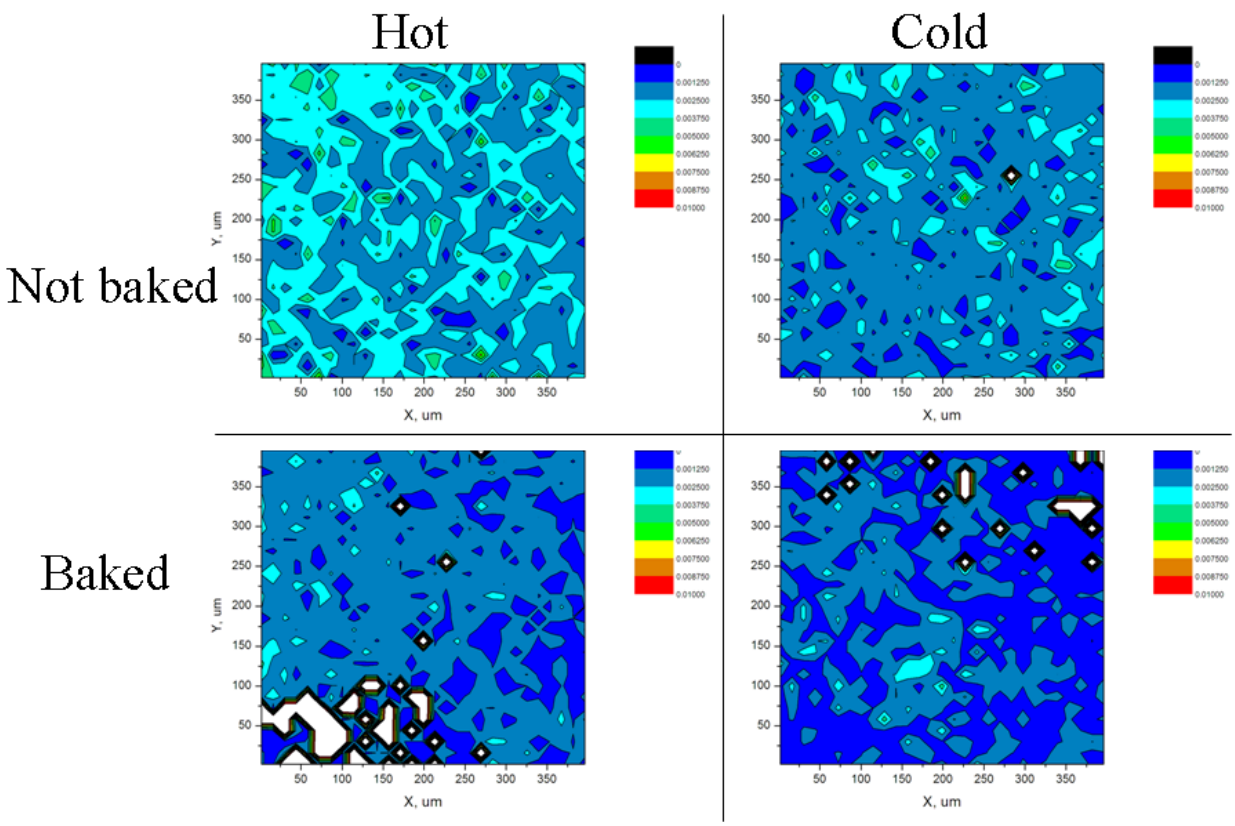

Figure 6: Average edge dislocation density (in arbitrary units) for hot (left column) and cold (right column) spots before (top row) and after (bottom row) mild baking.

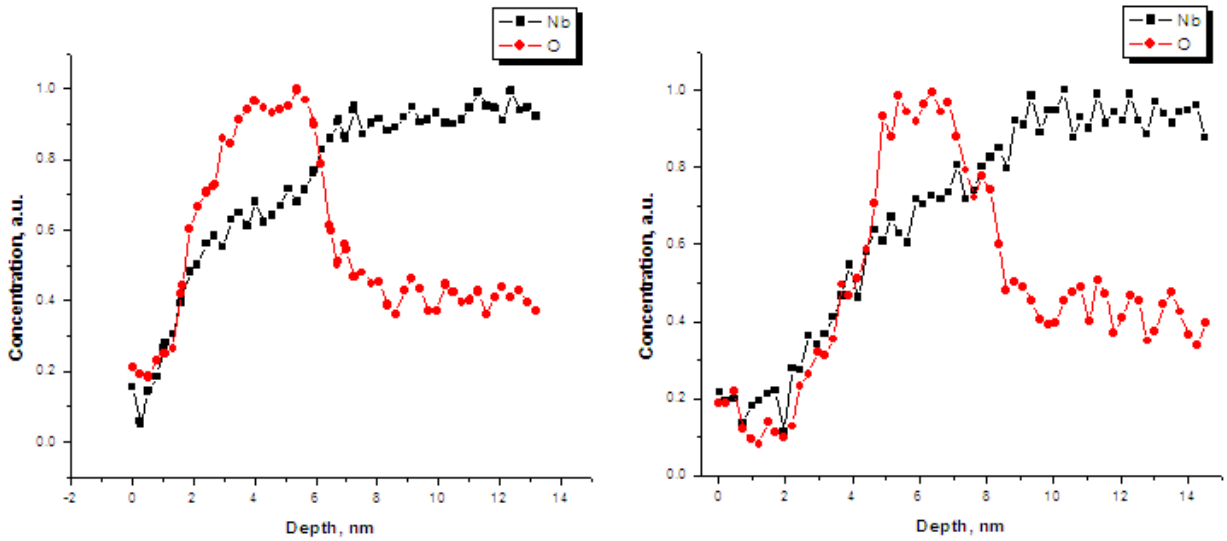

Figure 7: EELS depth profiles of Nb and O in small grain EP hot spot (left) and baked hot spot (right).

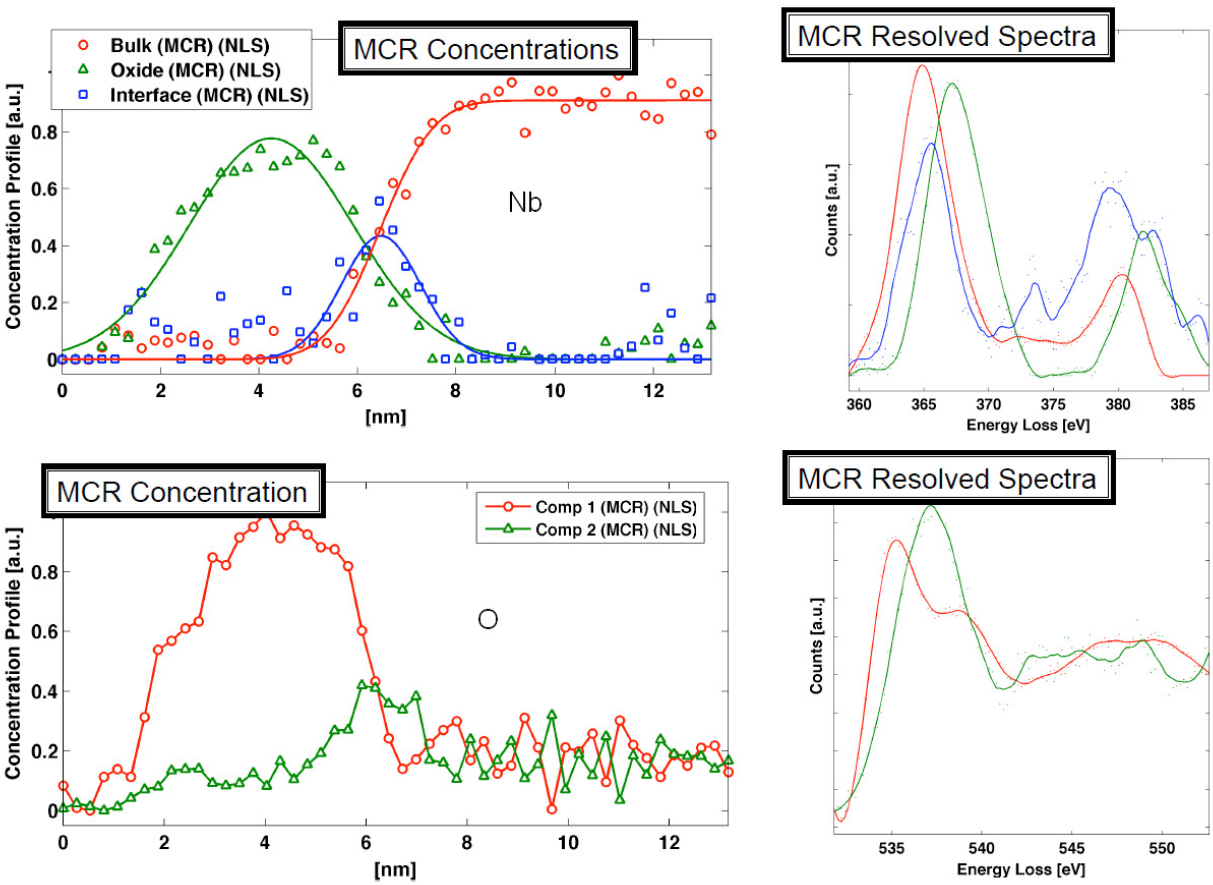

Figure 8: MCR decomposition of Nb (top) and O (bottom) EELS signals for the hot spot sample (by J. Mundy).

DISCUSSION

Dislocations

Crystalline orientation data on hot and cold spots before and after mild baking indicates that dislocations might be involved in both an emergence of the HFQS and the HFQS elimination by mild baking. Magnitudes of local misorientation shifts for hot/cold spots are consistent with the relative intensities of losses in hot/cold spots in cavities of different grain size and surface treatment. An exact

mechanism of how dislocations affect an RF superconductivity is not clear but there are two apparent possibilities. Firstly, dislocations serve as scattering centers for Cooper pairs, effectively reducing a local coherence length ξ. This in turn translates into an increase of the Ginsburg-Landau parameter κ and a decrease of the first critical field H_{c1}. Therefore, magnetic flux penetration can start at lower surface magnetic fields compared to pristine niobium, which might be the reason for the HFQS and stronger losses at hot spots. Second possibility is that the presence of dislocations suppresses the Bean-Livingston surface barrier for the fluxoid penetration due to an attractive interaction fluxoid-dislocation. The lowered surface barrier results in the lower superheating field causing fluxoids to start penetration at lower fields. Since individual dislocations are two small compared to the coherence length $\xi = 40\ nm$, it is more likely that dislocation pileups in dislocation cell walls serve as magnetic field penetration sites rather than individual dislocations. Dislocation cell structure suggested by calculated dislocation density maps (Fig. 5- 6) has a characteristic cell size of a few tens of micrometers.

The presence of fluxoids inside niobium within the RF magnetic field penetration depth causes dissipation, which consists of two components:

- Inductive losses due to the stationary fluxoid normal conducting core originating from the superconducting current time variation
- Losses due to the fluxoid motion arising from the viscous drag

In order to estimate the magnitude of additional dissipation due to magnetic flux present inside niobium, we use a simplified model of Rabinowitz [6]. Under assumptions of negligible fluxoid mass, image force and pinning force the resulting effective surface resistance is $R_{flux} = 4\ mOhm$. The surface density of fluxoids needed for cavity quality factor Q_0 to decrease by a factor of two at $H_{peak} = 100\ mT$ is then $\sigma_{flux} \approx 5 \times 10^8 m^{-2}$, and the average distance between fluxoids is $d_{flux} = \frac{1}{\sqrt{\sigma_{flux}}} = 45\ \mu m$, which is comparable to the size of the cells seen in dislocation density maps.

Mild baking results in the significant decrease of both screw and edge dislocation densities (Fig. 5- 6), thereby reducing the number of premature flux entry sites. We suggest that this reduction might be the reason for the HFQS disappearance. An exact mechanism of dislocation density decrease might be due to dislocation climb. Since dislocation climb is a vacancy-assisted process, then in order for it to be possible, there should be mobile vacancies available in the material. In [7] it was shown by positron annihilation spectroscopy that in niobium the presence of hydrogen (which is inevitable in the near-surface region) results in the vacancies being bound in vacancy-hydrogen complexes, and the dissociation of vacancy-hydrogen complexes happens at about 100°C making vacancies mobile. Corresponding positron lifetime measurements from [7] are shown in Fig. 9. Empirically found temperatures for

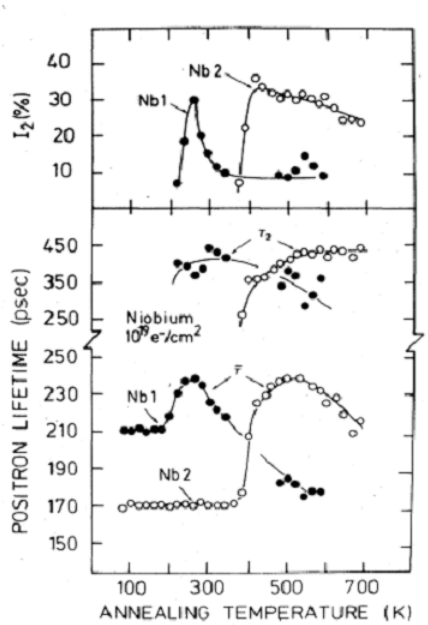

Figure 9: Positron lifetime data for Nb with (Nb1) and without (Nb2) hydrogen present from [7].

mild baking of niobium cavities are around exactly that temperature. Hence, the full mechanism, which we suggest as a possibility for mild baking is:

- Vacancies become mobile at about 100°C
- Dislocation climb is enabled by free mobile vacancies
- Dislocations rearrange with the decrease in total dislocation density

Oxide and Interface

TEM images and EELS elemental analysis show by direct observation that in samples from the HFQS-limited niobium cavities:

- Niobium oxide is uniform, and no suboxide clusters, cracks or other irregularities are present at the interface
- Niobium oxide structure is mostly Nb_2O_5 with a very thin suboxide layer resolvable only by detailed MCR analysis of the data; niobium oxide structure does not change due to mild baking followed by air exposure
- Interface between the oxide and bulk niobium is sharp and no extended layers of enriched oxygen content are present; no oxygen diffusion is observed due to mild baking

CONCLUSIONS

In summary, presence of regions with dense dislocations seem to be a plausible reason for the appearance of the HFQS in SRF niobium cavities. Mild baking effect might be due to decrease in dislocation density enabled by vacancy-assisted dislocation climb. Further studies on cavity-grade niobium dislocation and vacancy structures are planned to be performed.

ACKNOWLEDGEMENTS

The author would like to thank Hasan Padamsee for valuable discussions, John Grazul and Peter Ercius for TEM/STEM imaging, and Julia Mundy for EELS analysis. Cornell Center for Materials Research (CCMR) shared experimental facilities were used for data acquisition.

REFERENCES

[1] W. Pantleon, Scripta Materialia 58 (2008) 994997.

[2] D.P. Field et al., Ultramicroscopy 103 (2005) 3339.

[3] A. Romanenko et al., "Studies of the High Field Anomalous Losses in Small and Large Grain Niobium Cavities", SRF'07, Beijing, China, TUP24, http://jacow.org, 2007.

[4] A. Romanenko, Ph.D. Thesis, Cornell University, 2009.

[5] D. Bach et al., Microsc. Microanal. 13 (Suppl.2), 2007.

[6] M. Rabinowitz, Appl. Phys. Lett., 19(73), 1971; M. Rabinowitz, "Analysis of a critical loss in a superconductor", J. Appl. Phys., 88(42), 1971.

[7] P. Hautojarvi et al., Phys. Rev. B., Vol. 35, Num. 7, 1985.